ELSEVIER

Journal of Power Sources 90 (2000) 13–19

JOURNAL OF POWER SOURCES

www.elsevier.com/locate/jpowsour

Gelification of liquid–polymer systems: a valid approach for the development of various types of polymer electrolyte membranes

S. Panero, B. Scrosati *

Dipartimento di Chimica, Università ''La Sapienza'', 00185 Rome, Italy

Received 14 November 1999; accepted 31 January 2000

Abstract

Large interest is presently devoted to the development of gel membranes and to their use in advanced-design, plastic-like electrochemical devices. In our laboratory, we have demonstrated the validity of this approach for the case of lithium ion conducting membranes, e.g., membranes formed by the immobilization of mixed organic solutions of lithium salts in a polymer matrix (PM). Relevant examples are membranes formed by the gelification of a $LiPF_6$ ethylene carbonate–dimethyl carbonate (EC–DMC) solution into a poly(acrylonitrile) (PAN) matrix. In this paper, in addition to reporting the characteristics of some selected examples of lithium membranes, we demonstrate that the gel approach can be extended to other ion-conducting membranes. In particular, we report the properties of new types of protonic membranes formed by the inclusion of mixed solvent solution of an organic acid in a poly(methylmetacrylate) (PMMA) matrix. The results confirm that the gel-forming procedure, so far mainly addressed to the fabrication of lithium-conducting membranes, may indeed be extended to other ionic polymer systems. © 2000 Elsevier Science S.A. All rights reserved.

Keywords: Gelification; Liquid–polymer systems; Polymer electrolyte membranes

1. Introduction

In the present electrochemical technology, large interest is devoted to the substitution of common liquid solutions with ionically conducting membranes, which may serve both as electrolytes and separators. The idea is to develop advanced device configurations, where the conventional, liquid-like structure is changed into a plastic, flexible geometry. This applies to batteries (e.g., plastic lithium batteries), as well as to fuel cells (e.g., polymer electrolyte fuel cells), where the main goal is, in fact, replacing the liquid electrolyte by a polymer membrane.

This goal can only be successfully achieved if polymer membranes capable of combining a plastic consistency with properties similar to those of the liquids (e.g., high ionic conductivity and electrode compatibility) are available. There have been various attempts to characterize membranes of this type. One successful approach has been directed to the development of ''gel-type'' systems, namely, of electrolyte membranes formed by the gelification of liquid solutions in a polymer matrix (PM). These membranes were originally introduced in 1975 by Feullade and Perche [1], and were later further investigated by Abraham et al. [2,3] and Choe et al. [4], and more recently, extensively studied in our laboratory [5–11]. The most common application has been in lithium batteries by the development and characterization of membranes based on the gelification of lithium-conducting solutions. However, the approach is more general since, by properly defining the components and the preparation procedure, the gelification technique may be directed to different types of applications. Indeed, we think that gel-type membranes may be suitable for a variety of devices, which include lithium-conducting, as well as proton-conducting systems. In this paper, we report results confirming this assumption.

2. Experimental

The electrolyte membranes were generally prepared by gelling a liquid solution (LS) in a PM.

* Corresponding author. University of Rome, Piazzale Aldo Moro 5, 00185 Rome, Italy. Tel.: +39-6-4462866; fax: +39-491769.
E-mail address: scrosati@uniromal.it (B. Scrosati).

PII: S0378-7753(00)00438-9

In the case of lithium-conducting membranes, LS was a solution of a lithium salt (e.g., $LiClO_4$, $LiAsF_6$, $LiPF_6$, $LiN(SO_2CF_3)_2$, $LiC(SO_2CF_3)_3$, ...) in an organic solvent mixture (OSM; e.g., ethylene carbonate–propylene carbonate (EC–PC), ethylene carbonate–dimethyl carbonate (EC–DMC), ethylene carbonate–diethylene carbonate (EC–DEC), ...) and PM was a polymer of different type, such as poly(acrylonitrile) (PAN), poly(methylmethacrylate) (PMMA), poly(vinylidene)fluoride–hexafluoropropylene (PVdF–HFP) and poly(vinylidene) fluoride–chlorotrifluoro ethylene (PVdF–CTFE). The preparation procedure, specifically developed in our laboratory, involved a sequence of steps (all carried out inside an environmentally controlled dry-box), which included: (i) the dissolution at room temperature of the selected lithium salt (LiX) in the given OSM; (ii) the addition of the polymer component (PM) and its dispersion in the solution by stirring for several hours at room temperature; (iii) the very short (about 30 s) transfer of the formed slurry on an aluminum plate preheated at 90°C for promoting a fast and complete dissolution; and (iv) the cooling of the solution to room temperature to favour cross-linking in the membrane and gel formation.

This optimized synthesis procedure gives homogeneous and mechanically stable (free standing) membranes and greatly reduces the risk of decomposition phenomena. The membranes may be simply indicated by listing in sequence the components, e.g., LiX–OSM–PM. In our systematic research, we have considered various types of membranes formed by different combinations of their basic components and having an average thickness of 100 μm. The composition of some selected examples of these membranes is listed in Table 1.

The proton-conducting gel membranes were obtained by incorporating a highly plasticized PMMA matrix solutions of an organic acid (OA; e.g., salicylic acid (SA) or benzoic acid (BA)) in protophobic solvent mixtures (PSM; e.g., PC–EC) with low contents of protophilic solvents (PS; e.g., dimethylformamide (DMF), methylformamide (MF) or formamide (F)). The preparation procedure was conducted in a small glass reactor by careful addition at room temperature of the selected OA to the EC–PC solvent mixture to which the third PS solvent was incorporated. The complete OA dissolution was assured by prolonged mixing. Finally, PMMA was included in the solution by gradual addition at room temperature. Care was taken in order to prevent fast polymer dissolution and gel inhomogeneities. The mixture was then placed in a bath oil and the temperature was slowly increased up to 70°C and kept at this value under constant mixing for 45–60 min to promote the gel formation. The viscous mixture was finally placed between two teflon platelets to produce the gel membranes. The final products were stable and stored in open air. Table 2 lists the composition of some examples of the protonic gel membranes produced with this technique.

Table 2
Composition and conductivity (room temperature) of some examples of PMMA-based proton-conducting gel electrolyte membranes prepared in our laboratory (average thickness: 100 μm)

Membrane	Composition (mol%)	Conductivity (S cm^{-1})
BA, PC–EC, DMF, PMMA	8, 15–42, 5, 30	8.2×10^{-5}
SA, PC–EC, DMF, PMMA	5, 30–35, 5, 25	1.6×10^{-4}
SA, PC–EC, MF, PMMA	5, 30–35, 5, 25	2.5×10^{-5}
SA, PC–EC, F, PMMA	5, 30–35, 5, 25	1.8×10^{-4}

The ionic conductivity of all the membranes was measured by impedance spectroscopy run on cells formed by sandwiching the given sample between two stainless steel (SS) blocking electrodes in a button-type cell having an average surface area of 1 cm^2.

The electrochemical stability of the lithium-based gel-type membranes was evaluated by measuring their anodic

Table 1
Composition and conductivity (room temperature) of some selected examples of lithium-conducting gel electrolyte membranes prepared in our laboratory (average thickness: 100 μm)

Electrolyte membrane	Molar composition	Conductivity (S cm^{-1})	Anodic breakdown voltage vs. Li^+/Li^0 (V)
$LiClO_4$–EC–DMC–PAN	4.5–56.5–23.0–16.0[a]	3.9×10^{-3}	5.1
$LiClO_4$–EC–DEC–PAN	4.5–53.5–19.0–23.0[a]	4.0×10^{-3}	4.8
$LiAsF_6$–EC–PC–PAN	4.5–56.5–23.0–16.0[a]	0.9×10^{-3}	4.3
$LiPF_6$–EC–DMC–PAN	4.0–20.0–60.0–16.0[a]	5.9×10^{-3}	4.5–5.0
$LiN(SO_2CF_3)_2$–EC–PC–PAN	4.5–56.5–23.0–16.0[a]	1.0×10^{-3}	4.6
$LiClO_4$–EC–PC–PMMA	4.5–46.5–19.0–30.0[a]	0.7×10^{-3}	4.6
$LiAsF_6$–EC–PC–PMMA	4.5–46.5–19.0–30.0[a]	0.8×10^{-3}	4.8
$LiC(CF_3SO_2)_3$–EC–DMC–PAN	11.8–21.3–63–3.5	3.2×10^{-3}	4.3–4.5
$LiN(SO_2CF_3)_2$–EC–DMC–PMMA	5.0–50.0–20.0–25.0[a]	1.1×10^{-3}	4.8
$LiC(CF_3SO_2)_3$–EC–DBF–PVdF	3.5–36.5–30.0–30.0[a]	0.017×10^{-3}	–
$LiC(CF_3SO_2)_3$–EC–DBF–PVdF(C_3F_6)	3.5–36.5–30.0–30.0[a]	0.035×10^{-3}	4.8
$LiC(CF_3SO_2)_3$–EC–PC–PVdF(CTFE)	1.2–42.0–16.8–40.0[a]	0.1×10^{-3}	4.5

[a] This value is referred to monomer.

breakdown voltage. The latter was determined by running a low-scan (typically at 0.1 mV s^{-1} rate) sweep voltammetry in three-electrode cells using ''blocking-type'' working electrodes (e.g., stainless steel or nickel) lithium metal as both the counter and the reference electrode, and the given membrane sample as the electrolyte. The irreversible onset of the current in the anodic region was assumed as the given electrolyte's breakdown voltage.

3. Results and discussion

The conductivity of the membranes was measured by running an impedance analysis of cells formed by sandwiching the given sample between two blocking, stainless-steel electrodes. Fig. 1 shows a typical impedance response at room temperature for the case of a $LiPF_6$, EC, DMC, PAN lithium membrane, while Fig. 2 illustrates the related Arrhenius plot.

The results demonstrate that this, as well as the majority of the lithium membranes of this type (see Table 1), have a very high ionic conductivity which averages around 10^{-3}–10^{-2} at room temperature, i.e., approaching that of the corresponding liquid solutions. Furthermore, the shape of the impedance plot, which develops as a simple linear spike (Fig. 1), gives evidence of a good physical integrity of the membranes. In fact, lack in homogeneity, such as that induced by crystallization or phase separation phenomena, would have been reflected by semicircle evolution in the high impedance response. Further support for this conclusion is provided by (i) the absence of hysteresis between the heating and cooling scans (Fig. 2) and by (ii) the reproducibility of the impedance plots periodically detected upon prolonged storage time (Fig. 1). These experimental results confirm that the physical integrity and the homogeneity of the membranes are not affected either by thermal or by time excursions.

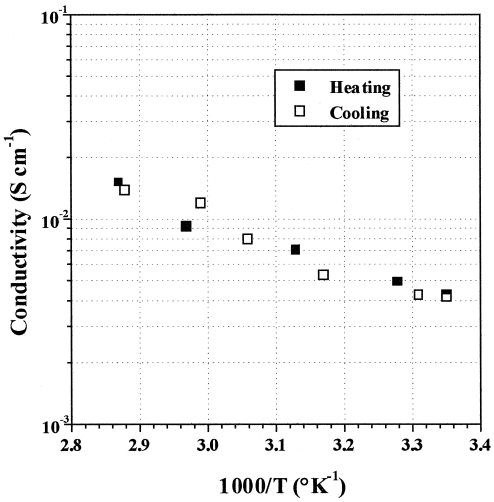

Fig. 2. Arrhenius plot of the $LiPF_6$, EC, DMC, PAN membrane. Data obtained by impedance analysis.

The electrochemical stability window of the lithium membranes was evaluated running a sweep voltammetry on a cell using a blocking, nickel-working electrode and a lithium counter electrode. A typical result, related to the $LiC(CF_3SO_2)_3$, PC, EC, PVdF membrane, is shown in Fig. 3. Three important features can be derived by this figure, namely, (i) the anodic onset of the current is detected around 4.5 V, which is assumed as the membrane decomposition voltage, i.e., a value high enough to allow a safe use of the membrane in connection with lithium ion electrode couples which typically cycle around 4 V [12]; (ii) the occurrence of a reversible cathodic peak around 0 V

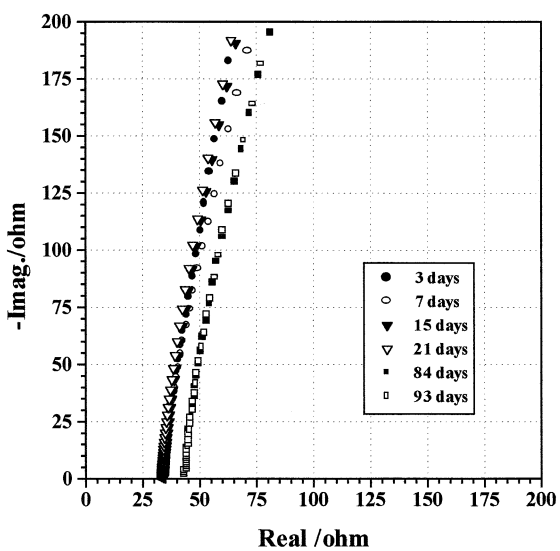

Fig. 1. Impedance response of a SS/$LiPF_6$, EC, DMC, PAN/SS cell at room temperature and at various storage times. Frequency range: 1 Hz–100 kHz.

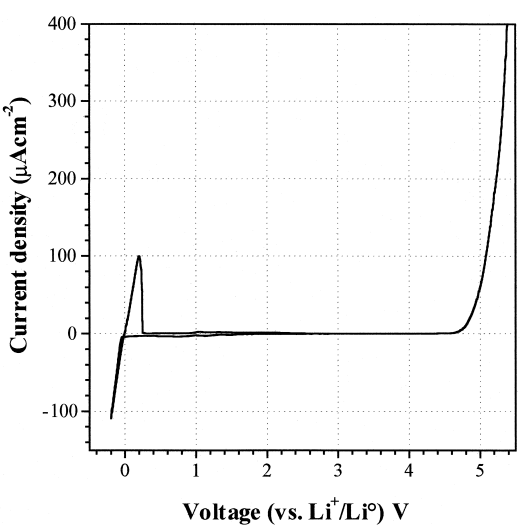

Fig. 3. Sweep voltammetry of a nickel electrode in a $LiC(CF_3SO_2)_3$, PC, EC, PVdF cell. Counter electrode: Li. Scan rate: 0.1 mV s^{-1}. Room temperature.

related to the lithium deposition-stripping process on the nickel substrate, which demonstrates the applicability of these membranes for lithium rechargeable batteries; and (iii) the very small residual current between the two limits, which is a clear evidence of the purity and of the integrity of the membranes.

The high and stable conductivity allows to suggest that although macroscopically solid, the gel-type membranes may benefit of a transport mechanism, which is similar to that of their liquid components. Indeed, recent results of dynamic light scattering measurements in PAN-based membranes confirm that the ionic conductivity of these membranes is closely related to the diffusive motion of the low molecular weight solvent mixture within the gel [13].

However, there is still some discussion whether the gel-type membranes are to be considered as simple two-phase systems where the polymer is a passive component acting as a rigid framework for regions of liquid solutions, or whether they are integrated systems where the polymer provides the stability of the gel network down to the immediate vicinity of the Li^+ ions. NMR [14,15] and Raman scattering [16,17] studies of membranes having different LiX–OSM–PM composition and nature have shown the influence of the PM in promoting ion–solvent interactions in the gels. For instance, in the case of a membrane using a PAN matrix, there are clear evidences of a strong coordination of the solvated ions and the solvent molecules, whereas in those using the PMMA matrix, the interaction is weak. Thus, while the PMMA-based systems can be regarded as electrolytes embedded in a ''passive'' host polymer, the PAN-based systems give clear evidence of an ''active'' polymer with strong polymer–electrolyte interactions.

These results allow to conclude that the gel procedure is particularly suitable for the fabrication of lithium-conducting membranes having high ionic conductivity, mechanical stability and physical integrity, which, in some cases, is also induced by specific interactions between the components. These properties make the membranes of definite interest for practical applications in the lithium metal and lithium ion advanced battery technology. Indeed, the recent trends of this technology are oriented towards the conversion of the present liquid-like configuration into gel-based polymer structures for the production of new-design, thin-film batteries addressed to the consumer electronics market [18].

The question is whether this procedure is limited to the lithium case or may be successfully extended to other ion-conducting systems. In this respect, one may consider that ionic transport in cross-linked swollen polymers containing a low molecular weight polar or ion-chelating additive may indeed occur in the solvent phase, and thus, the gel-concept can be extended to various alternative systems, including the proton-conducting systems. Indeed, proton-conducting polymeric gel or hydrogel membranes with conductivity values around 10^{-3} S cm^{-1} have been developed in the past [19,20]. We have extended the series by considering gel membranes formed by including organic acids (e.g., BA or SA) into a PMMA matrix [21]. This is an interesting approach to develop novel proton-conducting gel membranes having transport properties not dramatically depending on the humidity level. In fact, the carboxylic groups are expected to be able to act as proton donors and to show low levels of hydration, while the ring itself is rather non-polar. In addition, the melting point of these acid molecules is generally higher than the boiling point of water, which makes them interesting candidates for supporting high proton conductivity at room temperature.

The chemical stability of these PMMA-based protonic membranes was controlled by combined Differential Gravimetric Analysis and Thermal Gravimetric Analysis,

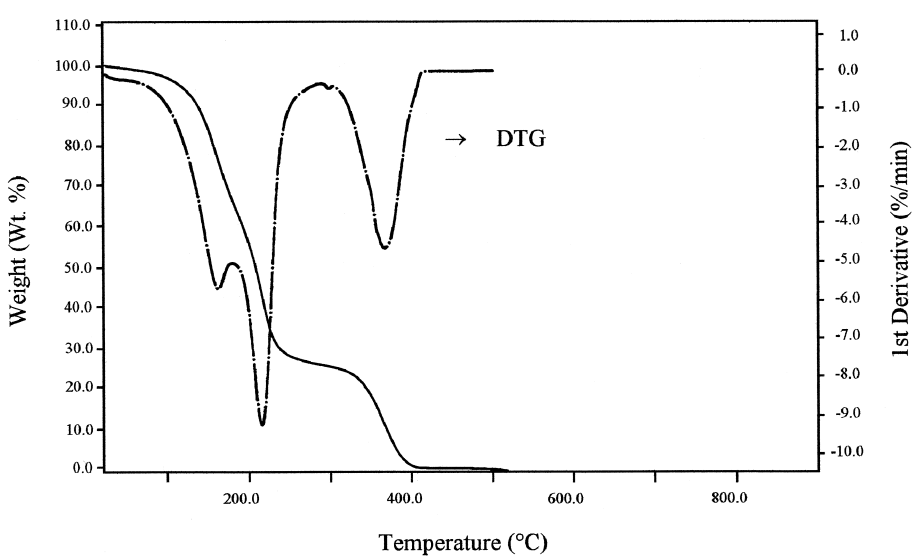

Fig. 4. TGA and DTG curves for the SA, PC–EC, DMF, PMMA membrane. Heating rate: 10°C/min under nitrogen.

DTG/TGA. Fig. 4 shows the results for the case of the SA, PC–EC, DMF, PMMA membrane. The trend of the curve reveals the weight loss of SA (around 160°C) and the solvent mixture evaporation (around 215°C). The process at 370°C corresponds to the PMMA degradation. In general, the thermal stability of these membranes can be assumed to be good up to 70–90°C. Fig. 5 shows the result of a gravimetric analysis of the BA, PC–EC, DMF, PMMA membrane. In this case, the stability is higher, i.e., extending over 100°C.

Fig. 6 shows the impedance plot obtained for the SA, PC–EC, DMF, PMMA membrane, showing the straight linear behaviour expected by the response of blocking electrodes. Again, as in the lithium systems, no interfacial contribution to the overall conductivity is revealed, confirming the integrity of the membranes, which were featured as robust electrolyte systems.

Fig. 7B shows the Arrhenius plot of the liquid electrolytes used to prepare the SA-based membranes. It can be noticed that full dissolution of SA in the plain PC–EC solvent mixture could only be obtained at temperatures higher than 60°C. In contrast, the protophilic nature of DMF, MF or F, allows to extend the complete dissolution at room temperature. It is also important to remark that the conductivity values of the membranes are higher than those of the plain solutions, as can be clearly seen from Fig. 7A, which reports the Arrhenius plot of the SA-based membranes: the conductivity values for samples containing F, MF and DMF are one order of magnitude higher than those of samples containing PC–EC only (see also Table 2).

This effect can, in part, be attributed to a specific interaction between the polymer and the non-polar fragment of the SA molecule, thus, enhancing ionic transport. In addition, one may assume that DMF, MF or F induces a more polar environment inside the gel matrix due to their strongly polar amide groups. These groups, in the presence of strong acids, essentially produce NH_4^+ cations. Also, there are evidences of important modifications in the elec-

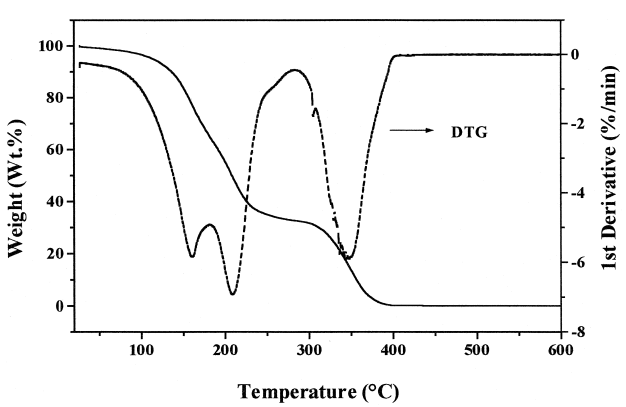

Fig. 5. TGA and DTG curves for the BA, PC–EC, DMF, PMMA membrane. Heating rate: 10°C/min under nitrogen.

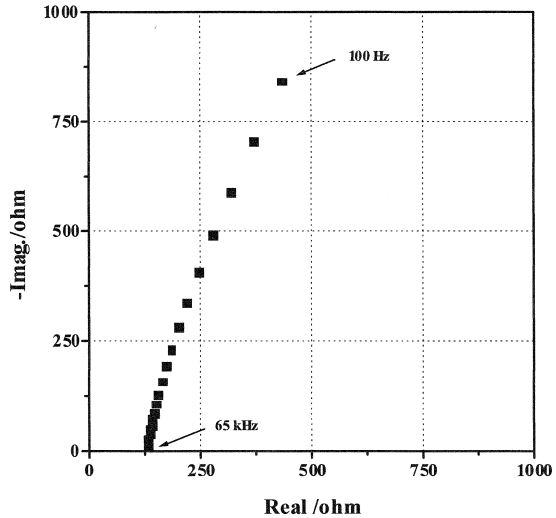

Fig. 6. Impedance response of a SS/SA, PC–EC, DMF, PMMA/SS cell. Frequency range: 100 Hz–65 kHz.

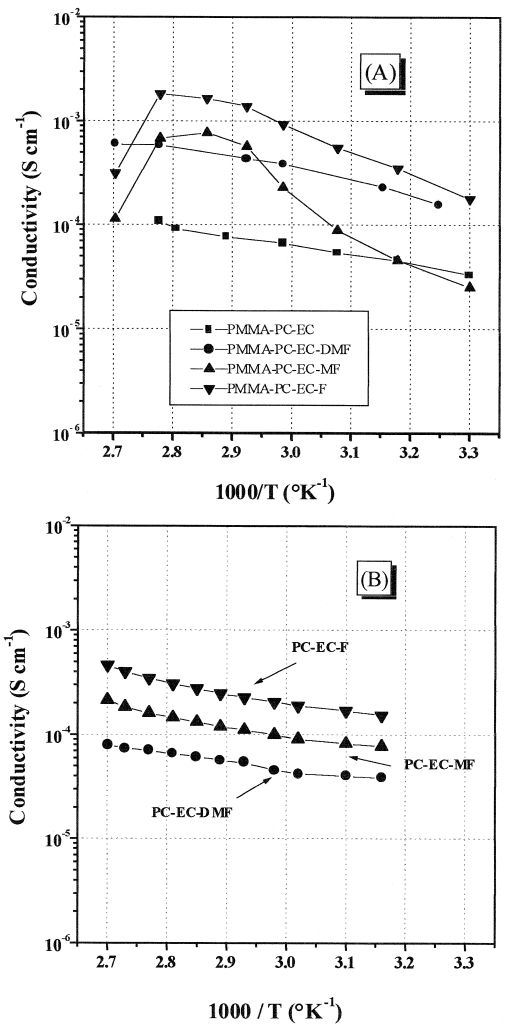

Fig. 7. Arrhenius plots of the SA-based PMMA membranes (A) and of their corresponding liquid solutions (B). Data derived from impedance analysis.

tronic distribution of C=O and C−N bonds depending on the polarity of the medium [22]. These considerations may somewhat account for the conductivity behaviour observed with DMF-, MF- or F-added membranes. Indeed, Raman studies support this explanation. Fig. 8 shows the Raman spectra of BA- and SA-based membranes with and without DMF addition. The differences in the related Raman shifts are quite clear in showing the effect of DMF in promoting acid dissociation.

On the other hand, one has to point out that the SA-based membranes containing MF show an unusual non-linear conductivity response reaching a maximum of around 80°C. This maximum is followed by a rapid decay at higher temperatures. A similar conductivity response is also shown by the F-containing membranes. This behaviour, which is in accordance with the DTG/TGA results (Fig. 4), can be explained in terms of high chemical reactivity of the membrane components at temperatures exceeding 70°C. In fact, membranes containing DMF, MF and F, respectively, which have been annealed at 100°C for 24 h, showed a remarkable conductivity loss. Thus, one may conclude that the DMF–MF or F-containing SA-based based systems are stable only at temperatures below 70°C.

Fig. 9 shows the Arrhenius plot of a typical BA-based membrane. To be noticed the high value of the room temperature conductivity (of the order of 10^{-4} S cm^{-1}, see also Table 2) and the decay at 100°C reflecting the lack of stability of the membrane over this temperature limit (see also Fig. 5).

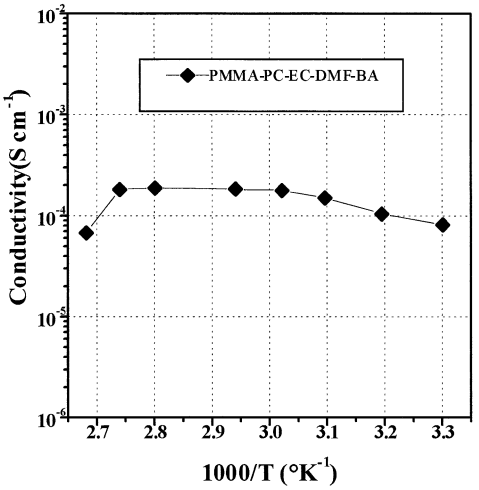

Fig. 9. Arrhenius plots of the BA-based PMMA membranes. Data derived from impedance analysis.

Fig. 10 shows the effect of the environmental humidity on the conductivity of SA-based PMMA membranes compared with that of a typical Nafion membrane, i.e., the presently most used proton-conducting membrane. The result confirms the expectations of a transport mechanism

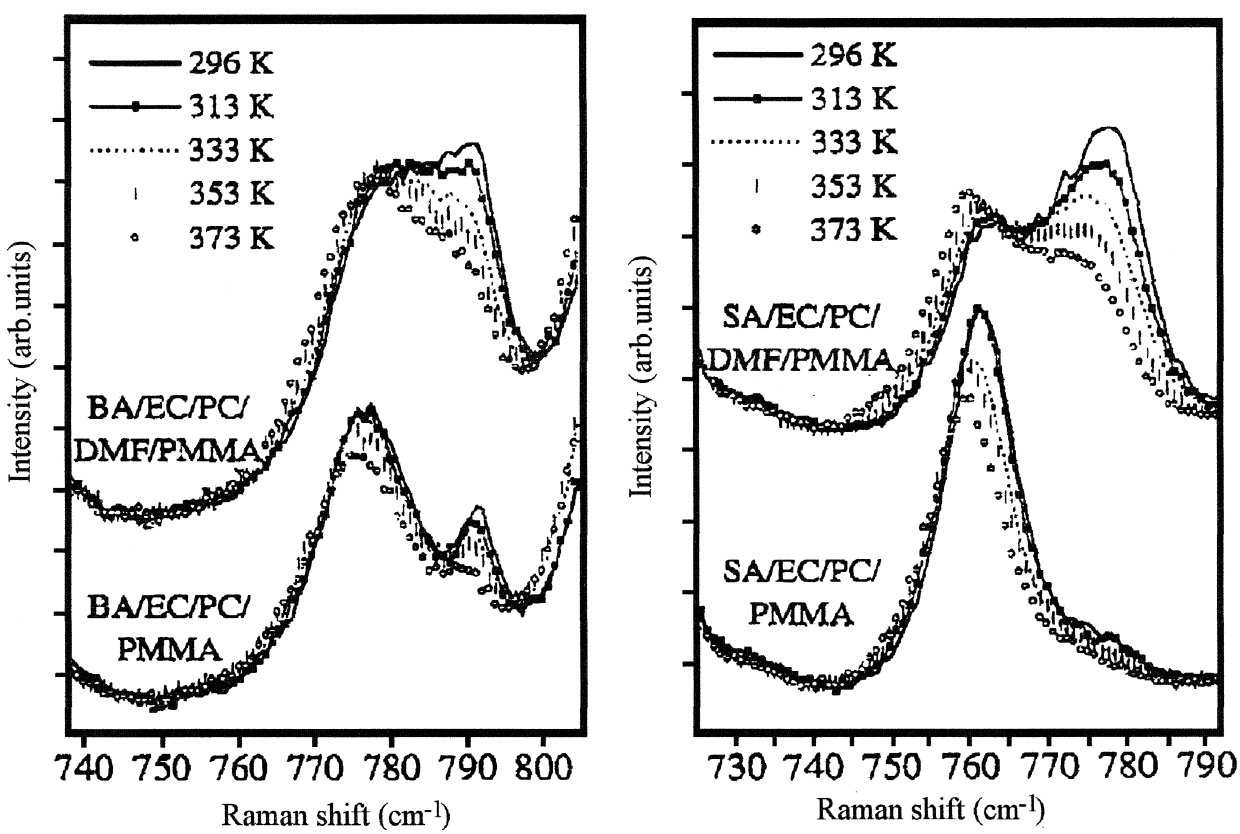

Fig. 8. Raman spectra of BA- and SA-based PMMA membranes with and without the addition of the DMF component.

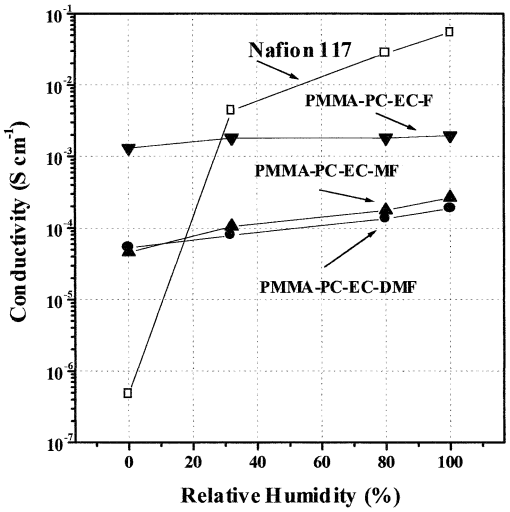

Fig. 10. Influence of the humidity content on the conductivity of PMMA-based, SA-type membranes in comparison with that of a Nafion 117 membrane (12 mm in diameter, about 0.17 mm in thickness).

in PMMA membranes, which is not dramatically influenced by the humidity level.

4. Conclusion

The results reported in this work supports the prevision that the gel-forming procedure, so far mainly exploited for the fabrication of lithium membranes, can be extended to other ion-conducting electrolytes as well. In particular, we show that by the proper selection of the acid and solvent components, protonic membranes with good transport properties may be obtained. Tests on the applicability of these new types of membranes are underway in our laboratory.

Acknowledgements

The authors wish to thank H. Andersson of Chalmers University of Technology, Sweden for the Raman measurements. Financial support from the Italian Ministry for University and Scientific Research, MURST-cofinanziamento 1998, is acknowledged.

References

[1] G. Feuillade, Ph. Perche, J. Appl. Electrochem. 5 (1975) 63.
[2] K.M. Abraham, R. Neat, B. Scrosati, in: B. Scrosati (Ed.), Applications of Conductive Polymers, Chapman & Hall, London, 1993, p. 182.
[3] K.M. Abraham, H.S. Choe, D. Pasquariello, Electrochim. Acta 43 (1998) 2399.
[4] H.S. Choe, B.G. Carroll, D.M. Pasquariello, K.M. Abraham, Chem. Mater. 9 (1997) 369.
[5] G. Dautzenberg, F. Croce, S. Passerini, B. Scrosati, Chem. Mater. 6 (1994) 538.
[6] G.B. Appetecchi, G. Dautzenberg, B. Scrosati, J. Electrochem. Soc. 143 (1996) 6.
[7] G.B. Appetecchi, F. Croce, G. Dautzenberg, F. Gerace, S. Panero, F. Ronci, E. Spila, B. Scrosati, Gazz. Chim. Ital. 126 (1996) 405.
[8] G.B. Appetecchi, F. Croce, B. Scrosati, J. Power Sources 66 (1997) 77.
[9] G.B. Appetecchi, F. Croce, A. De Paolis, B. Scrosati, J. Electroanal. Chem. 463 (1999) 248.
[10] G.B. Appetecchi, F. Croce, P. Romagnoli, B. Scrosati, U. Heider, R. Oesten, Electrochem. Commun. 1 (1999) 83.
[11] G.B. Appetecchi, F. Croce, R. Marassi, L. Persi, P. Romagnoli, B. Scrosati, Electrochim. Acta, in press.
[12] S. Megahed, B. Scrosati, J. Power Sources 51 (1994) 79.
[13] C. Svanberg, J. Adebahr, H. Ericson, L. Borjesson, L.M. Torell, B. Scrosati, J. Chem. Phys, in press.
[14] P.E. Stallworth, S.G. Li, S.G. Greenbaum, F. Croce, S. Slane, M. Salomon, Solid State Ionics 73 (1994) 119.
[15] C.A. Edmonson, M.G. Wintersgill, J.L. Fontanella, F. Gerace, B. Scrosati, S.G. Greenbaum, Solid State Ionics 85 (1996) 173.
[16] D. Ostrovski, L. Torrell, G.B. Appetecchi, B. Scrosati, Solid State Ionics 106 (1998) 19.
[17] O. Ostrovskii, A. Brodin, L.M. Torell, G.B. Appetecchi, B. Scrosati, J. Phys. Chem. 109 (1998) 7618.
[18] T. Osaka, Interface (1999).
[19] J. Przyluski, W. Wieczorek, Synth. Met. 45 (1991) 323.
[20] J.R. Stevens, W. Wieczorek, D. Raducha, K.R. Jeffrey, Solid State Ionics 97 (1997) 347.
[21] A.M. Grillone, S. Panero, B.A. Retamal, B. Scrosati, J. Electrochem. Soc. 146 (1999) 27.
[22] G. Vaivars, J. Kleperis, A. Azens, C.G. Granqvist, A. Lusis, Solid State Ionics 97 (1997) 365.